Thermochimica Acta 564 (2013) 51–58

Contents lists available at SciVerse ScienceDirect

Thermochimica Acta

journal homepage: www.elsevier.com/locate/tca

Investigation of synthesis, thermal properties and curing kinetics of fluorene diamine-based benzoxazine by using two curing kinetic methods

Xuan-yu He [a], Jun Wang [a], Noureddine Ramdani [a], Wen-bin Liu [a,*], Li-jia Liu [a], Lei Yang [b]

[a] Polymer Materials Research Center, College of Materials Science and Chemical Engineering, Harbin Engineering University, Harbin 150001, China
[b] Key Laboratory of Forest Plant Ecology, Ministry of Education, Northeast Forestry University, Harbin 150040, China

ARTICLE INFO

Article history:
Received 7 December 2012
Received in revised form 10 April 2013
Accepted 20 April 2013
Available online 3 May 2013

Keywords:
Fluorene diamine-based benzoxazine
Polymerization behavior
Curing kinetics
Thermal properties

ABSTRACT

A novel diamine-based benzoxazine monomer containing aryl ether and bulky fluorene groups (BEF-p) was prepared from the reaction of 9,9-bis-[4-(*p*-aminophenoxy)-phenyl]fluorene with paraformaldehyde and phenol. The chemical structure of monomer was confirmed by Fourier-transform infrared (FTIR) and ^{1}H and ^{13}C nuclear magnetic resonance spectroscopy (^{1}H and ^{13}C NMR). The polymerization behavior of monomer was analyzed by differential scanning calorimetry (DSC) and FTIR. The curing kinetics was studied by non-isothermal DSC, and the kinetic parameters were determined. The autocatalytic model based on two kinetic methods (Starink-LSR method and direct LSR method) showed good agreement with experimental results. The thermal and mechanical properties of poly(BEF-p) were evaluated with DSC, dynamic mechanical thermal analysis (DMTA), and thermogravimetric analysis (TGA). The results showed that the cured polymer exhibited higher glass transition temperature (T_g) and better thermal stability compared with diaminodiphenylmethane-based benzoxazine(P-ddm), and was slightly lower than those of fluorene diamine-phenol-based polybenzoxazine (poly(BF-p)).

1. Introduction

Polybenzoxazines, as a class of thermosetting phenolic resins formed by the cationic ring-opening of the corresponding benzoxazine monomers without any added initiator, have demonstrated various attractive properties such as high thermal stability, high char yields, high glass transition temperature (T_g), near-zero volumetric change upon curing, good mechanical and dielectric properties, low water absorption, and low flammability. These unique characteristics make the polybenzoxazines a better candidate over epoxies and traditional phenolic resins in the electronics, aerospace, and other industries [1–5]. According to the related researches, most difunctional benzoxazines were synthesized from bisphenols, monoamines, and formaldehyde. The large varieties of aromatic bisphenols and monoamines allow for considerable molecule-design flexibility of benzoxazines [6–12]. Another series of important difunctional benzoxazines were the diamine-based benzoxazines. Allen and Ishida synthesized a series of aliphatic diamine-based benzoxazine monomers using monofunctional phenol with linear aliphatic diamines [13,14]. The polymerization behavior and curing kinetics of these monomers and thermal properties of their polymers were also discussed. Lin and coworkers successfully synthesized a series of aromatic diamine-based benzoxazines by the three-step, two-pot, or one-pot procedure [15–17]. Agag and Ishida et al. reported a new route for high yield synthesis of aromatic diamine-based benzoxazines using the one-step procedure, in which xylenes as a nonpolar, high-boiling-point solvent, was used at 150 °C [18]. Therefore, various difficult aromatic diamine-based benzoxazines can be prepared by different synthesis method [19–24]. Furthermore, the aromatic diamine-based polybenzoxazine can provide higher glass transition temperature and thermal stability than the conventional bisphenol-A-based polybenzoxazine [25].

Fluorene molecular contains two benzene rings linked with a five-membered ring which can provide high overlaps of π-orbitals [26]. Incorporation of bulky pendant groups can impart a significant increase in both T_g and thermo-oxidative stability by restricting segmental mobility. Therefore, the development of these polymers has attracted extensive research interests during the past few years [27–33]. Recently, researches on synthesis, polymerization behavior, curing kinetics, and thermal properties of fluorene-based benzoxazines have been reported. Liu et al. prepared a series of fluorene-containing benzoxazines from the reaction of 9,9-bis-(4-hydroxyphenyl)-fluorene, aromatic and aliphatic primary amines, and formaldehyde [34]. Liu et al. also reported the preparation of a furan-terminated and fluorene-containing benzoxazine, and studied their properties [35]. Y.B. Lu et al. subsequently studied the curing kinetics of fluorene-based benzoxazines [36]. Xu et al. proved that hydrophobic characteristics of the fluorenyl-based

* Corresponding author. Tel.: +86 451 82589540; fax: +86 451 82589540.
E-mail address: wjlwb@163.com (W.-b. Liu).

0040-6031/$ – see front matter © 2013 Elsevier B.V. All rights reserved.
http://dx.doi.org/10.1016/j.tca.2013.04.024

polybenzoxazines are due to the low polarity of fluorenyl and π–π stacking interaction of fluorenyl on the surface [37]. Lin et al. reported the synthetic route of a benzoxazine based on 9,9-bis(4-aminophenyl) fluorene, 2-hydroxybenzaldehyde/phenol, and formaldehyde/paraformaldehyde by using two-pot and one-pot procedures, and studied the optical and thermal properties of the monomer and polybenzoxazines [38]. In our previous work, we also prepared a series of fluorene diamine-based benzoxazine monomers via the reaction of 9,9-bis-(4-aminophenyl)-fluorene with paraformaldehyde and unsubstituted or substituted phenols [39]. The polymerization behavior, regioselectivity, and thermal properties of monomers and cured polymers were discussed. However, their further applications were limited considerably due to brittleness of the formed polymers despite the advantageous properties of fluorene-based benzoxazines. The studies on performance enhancement of polybenzoxazine mainly include blending or alloying with other polymers and design of novel monomers with special properties. Some thermosetting resins such as polyimide, epoxy, cyanate ester and polyurethane resins have been blended with benzoxazine resins to improve the toughness of benzoxazine resins [40–43]. Another strategy is to prepare polybenzoxazines derived from bisphenol and linear aliphatic amine or phenol and linear aliphatic diamine which achieve high mechanical performance by incorporating a flexible chain into the polybenzoxazine matrix. However, the thermal properties of linear aliphatic amine-based polybenzoxazines generally exhibit low T_g and poor thermal stability, and decrease with the length of the aliphatic chains [13,14,44–46]. Introduction of flexible aryl ether linkages in the backbone is known to toughen polymers without significant reduction in thermal stability [47–51].

Curing process of benzoxazine resin is very complicated, which includes gelation, vitrification, subsequent crosslinking, and origination of three-dimensional networks. Therefore, the fundamental investigation of benzoxazine curing reaction kinetic is an attractive topic for a better understanding of the curing behavior as well as for the control and optimization of production processes and performance of final products [52]. DSC is based on a phenomenological method, in which kinetic analysis only need to calculate the heat variation for a whole reaction process with temperature or time, without distinguishing the individual reaction in the process. So DSC is the most utilized technique to determine kinetic parameters and rate equation of polymerization of benzoxazine [36,52–58].

In a continuation study on fluorene-based benzoxazine, the present work describes a successful preparation of diamine-based benzoxazine monomer without much sacrifice of thermal properties by incorporating aryl ether and bulky fluorene groups into the polymer backbone. Chemical structures of monomer were confirmed by FTIR, ^{1}H and ^{13}C NMR. The polymerization behavior and thermal properties of monomer and their cured polymer were discussed. Non-isothermal DSC was used to investigate the curing kinetics of BEF-p. Autocatalytic model, Starink method and the least square regression (LSR) method have been applied to calculate the kinetic parameters for cure reaction of BEF-p.

2. Experimental

2.1. Materials

9,9-bis-(4-Hydroxyphenyl)fluorene was synthesized according to literature [59]. *p*-Chloronitrobenzene, anhydrous potassium carbonate, hydrazine monohydrate, phenol and paraformaldehyde were obtained from Shanghai Jingchun Reagent Co., Ltd. (China). 10% palladium on activated carbon (Pd–C) was purchased from National Pharmaceutical Chemical Co., Ltd. (China). All solvents were purchased from Tianjin Kermel Chemical Reagent Co., Ltd. (China), and used without further purification.

2.2. Monomer synthesis

Scheme 1 illustrates the synthesis of 9,9-bis-[4-(*p*-nitrophenoxy)phenyl]fluorene (BNOFL), 9,9-bis-[4-(*p*-aminophenoxy) phenyl]fluorene (BAOFL) and BAOFL-based benzoxazine (BEF-p).

2.2.1. 9,9-bis-[4-(p-Nitrophenoxy)phenyl]fluorene (BNOFL)

A mixture of 9,9-bis-(4-hydroxyphenyl)fluorene (8.76 g, 0.025 mol), *p*-chloronitrobenzene (8.67 g, 0.055 mol), anhydrous potassium carbonate (7.95 g, 0.055 mol) and *N*,*N*-dimethylformamide (DMF, 80 mL) was refluxed for 8 h. The mixture was then cooled and poured into 400 mL of 1:1 ethanol-water. The precipitated powder were isolated by filtration and washed thoroughly with water. The product was dried under vacuum at 80 °C for 24 h. A yellow powder (94% yield, m.p. 333–335 °C) was obtained. FTIR (KBr, cm^{-1}): 1583 (NO_2 asymmetric stretching), 1338 (NO_2 symmetric stretching), 1249 (C—O—C asymmetric stretching), 846, 750 (C—H out-of-plane bending). ^{1}H NMR (500 MHz, $CDCl_3$, ppm): 6.95–8.19 (m, 24H, Ar—H). ^{13}C NMR (500 MHz, $CDCl_3$, ppm): 117.22–163.11 (36C, the carbons of benzene ring), 64.53 (1C, quaternary carbon in the fluorene ring).

2.2.2. 9,9-bis-[4-(p-Aminophenoxy)phenyl]fluorene (BAOFL)

Hydrazine monohydrate (60 mL) was added dropwise over a period of 1 h at 85 °C to a mixture of BNOFL (10.5 g, 0.018 mol), ethanol (150 mL), and a catalytic amount of Pd–C (0.2 g). After the addition was complete, the reaction was continued at reflux temperature for another 24 h, and the mixture was filtered to remove Pd–C. After cooling, white-needle crystals were isolated by filtration and washed thoroughly with ethanol. The yield was 81%; m.p. 177–178 °C. FTIR (KBr, cm^{-1}): 3477, 3366 (N–H stretching), 1234 (C—O—C asymmetric stretching), 873, 748 (C—H out-of-plane bending). ^{1}H NMR (500 MHz, $CDCl_3$, ppm): 6.62–7.74 (m, 24H, Ar—H), 3.55 (s, 4H, Ar—NH_2). ^{13}C NMR (500 MHz, $CDCl_3$, ppm): 116.21–157.69 (36C, the carbons of benzene ring), 64.28 (1C, quaternary carbon in the fluorene ring).

2.2.3. BAOFL-based benzoxazine (BEF-p)

BAOFL (10.6 g, 0.02 mol), phenol (3.8 g, 0.04 mol), paraformaldehyde (3.6 g, 0.12 mol) and 50 mL mixed isomer xylenes were added to a 150 mL three neck round-bottomed flask equipped with a magnetic stirrer, reflux condenser, and thermometer. The mixture was stirred at 150 °C for 6 h. After that, the reaction mixture was cooled to room temperature and then poured into hexane. The precipitated yellowish powder were isolated by filtration and washed thoroughly with ethanol and dried under vacuum. The product was dissolved in dimethylformamide (DMF), precipitated in 1 N aqueous solution of sodium hydroxide to remove any phenolic compounds, washed several times with water and finally with ethanol. The product was dried under vacuum at 60 °C for 24 h. Light yellow powder (82% yield) was provided. FTIR (KBr, cm^{-1}): 1370 (CH_2 wagging), 1224 (C—O—C asymmetric stretching), 1139 (C—N—C asymmetric stretching), 1067 (C—O—C symmetric stretching), 950 (C—H out-of-plane bending), 823, 747 (C—H out-of-plane bending). ^{1}H NMR (500 MHz, $CDCl_3$, ppm): 6.62–7.74 (m, 32H, Ar—H), 5.30 (s, 4H, O—CH_2—N), 4.58 (s, 4H, Ar—CH_2—N). ^{13}C NMR (500 MHz, $CDCl_3$, ppm): 116.93–156.79 (48C, the carbons of benzene ring), 80.16 (2C, O—CH_2—N), 64.35 (1C, quaternary carbon in the fluorene ring), 50.93 (2C, N—CH_2—Ar).

2.3. Curing of benzoxazine monomers

BEF-p was polymerized without initiator or catalyst according to the followings schedule: 180 °C/2 h, 200 °C/2 h, 220 °C/2 h and 240 °C/2 h in the air-circulating oven.

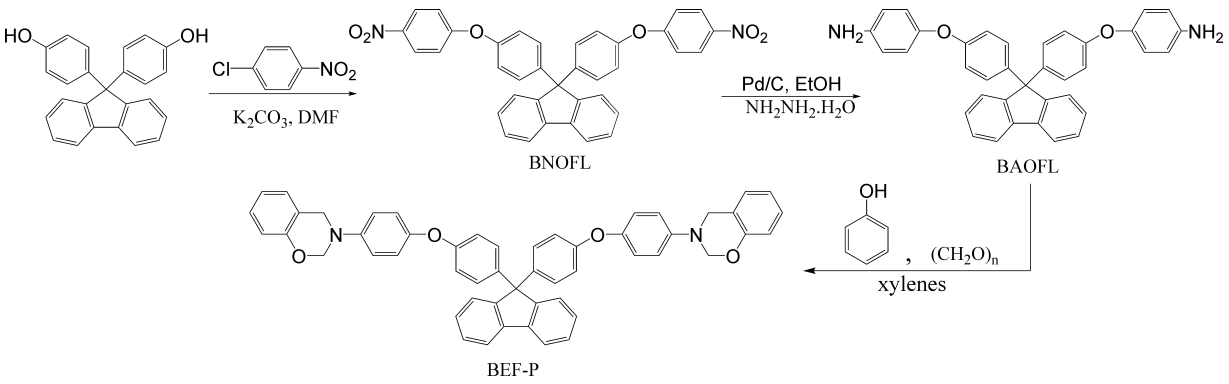

Scheme 1. The synthesis route of diamine-based benzoxazine monomer containing aryl ether and bulky fluorene groups (BEF-p).

2.4. Characterization

Fourier transform infrared (FTIR) spectra were recorded on a Perkin-Elmer Spectrum 100 spectrometer in the range of 4000–650 cm^{-1}, which was equipped with a deuterated triglycine sulfate (DTGS) detector and KBr optics. Transmission spectra were obtained at a resolution of 4 cm^{-1} after averaging two scans by casting a thin film on a KBr plate for monomers and cured samples. ^{1}H and ^{13}C NMR characterizations were performed on a Bruker AVANCE-500 NMR spectrometer using deuterated chloroform ($CDCl_3$) as the solvent and tetramethylsilane (TMS) as an internal standard. The average number of transients for ^{1}H and ^{13}C NMR is 32 and 1028, respectively. A relaxation delay time of 1s was used for the integrated intensity determination of ^{1}H NMR spectra. DSC measurements were evaluated on a TA Q200 differential scanning calorimeter under a constant flow of a nitrogen atmosphere of 50 mL/min. The instrument was calibrated with a high-purity indium standard, and α-Al_2O_3 was used as the reference material. About 5 mg of sample was weighed into a hermetic aluminum sample pan at 25 °C, which was then sealed, and the samples were scanned by the non-isothermal method from 20 to 350 °C using 5, 10, 15 and 20 °C/min heating rate under nitrogen. Thermogravimetric analysis (TGA) was performed on TA Instruments Q50 at a heating rate of 20 °C/min from 30 to 800 °C under nitrogen atmosphere at a flow rate of 50 mL/min. The dynamic mechanical thermal properties of the obtained polybenzoxazines were carried out with a TA Q800 dynamic mechanical analyzer. The rectangular samples (20 mm × 5 mm × 2 mm) were loaded in single cantilever mode at a temperature ramp of 3 °C/min from 30 to 300 °C with a frenquency of 1 Hz under air atmosphere.

3. Results and discussion

3.1. Synthesis and structure of the benzoxazine monomers

The diamine 9,9-bis-[4-(*p*-aminophenoxy)phenyl]fluorene (BAOFL) was synthesized in two steps from 9,9-bis-(4-hydroxyphenyl)fluorene [47]. The dinitro compound BNOFL was prepared by nucleophilic substitution reaction from 9,9-bis-(4-hydroxyphenyl)fluorene with *p*-chloronitrobenzene in the presence of anhydrous potassium carbonate. The catalytic hydrogenation of BNOFL to the diamine BAOFL was accomplished by means of hydrazine monohydrate as well as a catalytic amount of Pd–C. The IR spectrum of BNOFL showed characteristic absorptions for nitro groups at 1583 and 1338 cm^{-1}. After hydrogenation, the characteristic absorptions of BNOFL disappeared. New absorptions at 3477 and 3366 (N—H stretching) appeared. Moreover, the structure of BAOFL was further identified by NMR spectroscopy

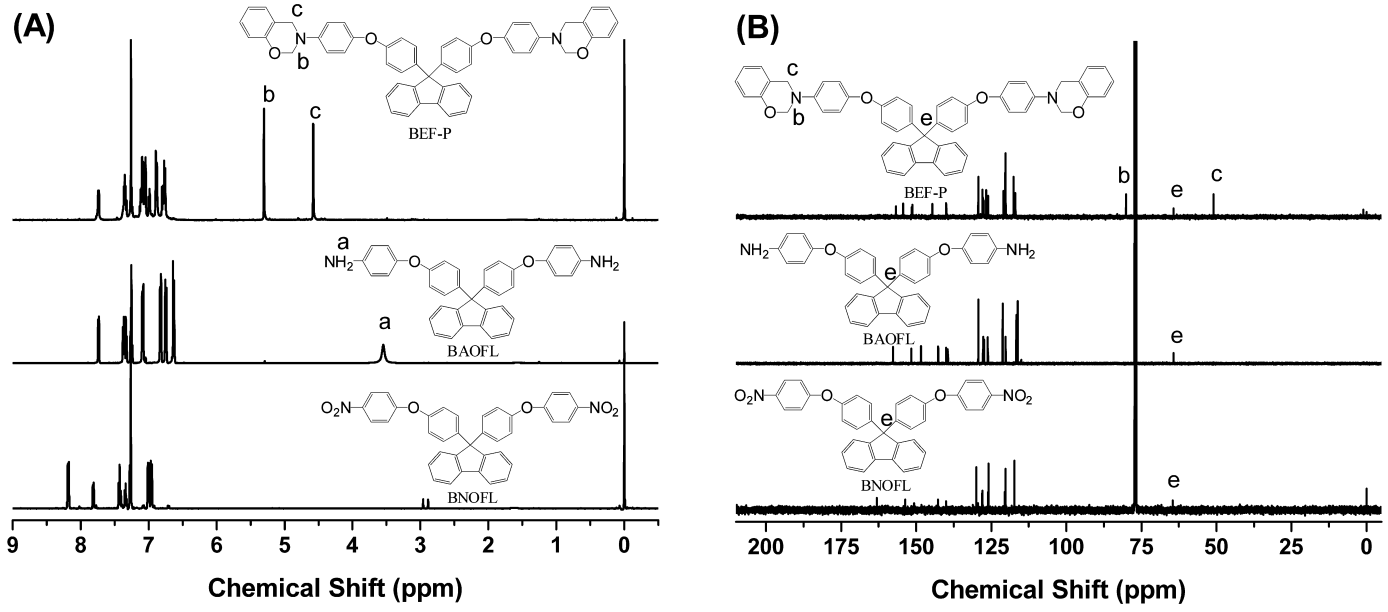

Fig. 1. ^{1}H NMR (A) and ^{13}C NMR (B) spectra of BNOFL, BAOFL and BEF-p.

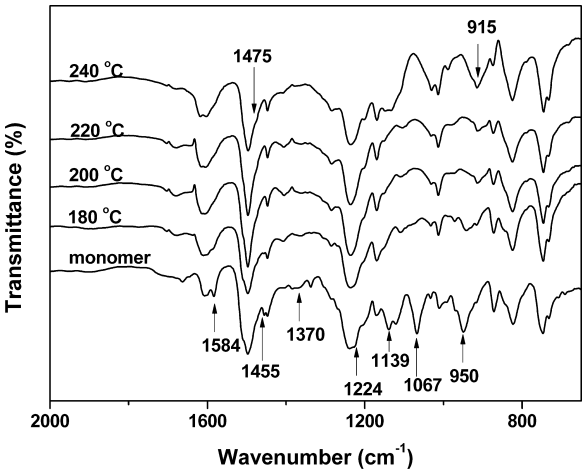

Fig. 2. FT-IR spectra of BEF-p at each cure stage.

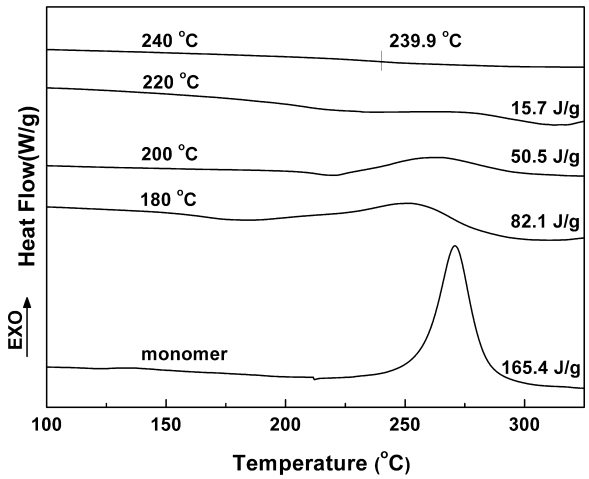

Fig. 3. DSC thermograms of BEF-p at each cure stage.

as shown in Fig. 1. These results clearly confirm that the diamine prepared herein is the proposed structure.

The synthesis of BEF-p was accomplished using the one-step procedure [18]. The formation of oligomers as a result of the polymerization of formed benzoxazine was minimal. This ensures that the benzoxazine monomer synthesized has a high purity, which is recommended to facilitate the studies of polymerization behavior and curing kinetics. The ^{1}H and ^{13}C NMR spectra were also recorded to confirm the structure (Fig. 1). In ^{1}H NMR spectrum (Fig. 1(A)), the aromatic protons are observed at 6.62–7.74 ppm. The chemical shifts at 5.30 and 4.58 ppm are attributed to methylene (O—CH_2—N) and methylene (Ar—CH_2—C) of oxazine ring, respectively. In ^{13}C NMR spectrum (Fig. 1(B)), the resonances at 116.93–156.79 ppm are assigned to the aromatic carbon atoms. The chemical shifts at 50.93 and 80.16 ppm are ascribed to the carbon atom resonances of N—CH_2—Ar and O—CH_2—N of oxazine rings, respectively. The signals located at 64.35 ppm are due to the presence of quaternary carbon atoms in the fluorene structure [34]. The NMR results confirmed the successful synthesis of BEF-p.

FT-IR spectrum of BEF-p monomer is shown in Fig. 2. The absorption band assigned to the out-of-plane bending vibrations of C—H located at 950 cm^{-1} is due to presence of the characteristic mode of benzene with an attached oxazine ring [24,34]. The absorptions located at 1224 cm^{-1} and 1067 cm^{-1} are corresponding to the asymmetric and symmetric stretching vibrations of C—O—C, respectively. The band at 1139 cm^{-1} is attributed to the asymmetric stretching vibrations of C—N—C [60]. The absorption bands at 823 and 747 cm^{-1} are attributed to the C—H out-of-plane bending mode of the *para* and *ortho* disubstituted benzene of aniline, aryl ether, and fluorene ring in BAOFL skeleton, respectively. The CH_2 wagging in the oxazine ring is located at 1370 cm^{-1} [15,18]. Furthermore, the characteristic absorption bands of *ortho*-disubstituted benzene appear at 1584 cm^{-1} and 1455 cm^{-1}, as well as 750 cm^{-1} [13].

3.2. Polymerization behavior of BEP-p

The polymerization behavior of BEP-p was investigated by DSC and FTIR. The obtained FTIR spectra and non-isothermal DSC thermograms of BEF-p at each cure stage are shown in Fig. 2 and Fig. 3, respectively. As can be seen from Fig. 2, as the curing temperature increases, the characteristic absorption bands associated with the oxazine ring at 950 cm^{-1}, CH_2 wagging at 1370 cm^{-1}, the asymmetric and symmetric stretching vibrations of C—O—C at 1224 and 1067 cm^{-1} and C—N—C at 1139 cm^{-1}, respectively, gradually decrease. At 240 °C, the characteristic peaks completely disappear, indicating the completion of ring-opening in this stage. Meanwhile, the very strong band assigned to the symmetric stretching modes of C—N—C around 915 cm^{-1} appears. These suggest that the crosslinking reaction further performs and the crosslink density of polybenzoxazine increases by the ring-opening polymerization at elevated temperature. The absorptions at 1584 and 1455 cm^{-1} assigned to the *ortho*-disubstituted benzene ring of benzoxazine monomer shift to around 1475 cm^{-1} due to the formation of tetrasubstituted benzene ring after thermal curing [13,19]. This result indicates that the crosslinking reaction for BEF-p might also occur at *para* position on the phenol besides the *ortho* position during thermal curing.

As can be seen in Fig. 3, the amount of exotherm gradually decreases with the increase of heat-treatment temperature, and the degree of curing gradually increases. From Fig. 3 it may be observed that the uncured monomer exhibits an exothermal peak at 271 °C assigned to the monomer polymerization. If the monomer was previously cured at 180 °C or 200 °C before the DSC tests, the polymerization process is accelerated probably due to the already formed OH groups into the polymer chain so that the peak temperature is shifted to lower temperature [58]. When the sample is cured at 180 °C, 200 °C, and 220 °C, the degree of curing attains 50.4%, 69.5%, and 90.5%, respectively. However, the exothermic peak completely disappears at 240 °C, implying that the polymerization reaction is completed. The step change of the thermogram assigned to the glass transition temperature (T_g) can be observed in this stage.

3.3. Curing kinetics

The curing kinetics analysis is based on the rate Eq. (1) [61]:

$$\frac{d\alpha}{dt} = \beta\frac{d\alpha}{dT} = k(T)f(\alpha) \quad (1)$$

where $k(T)$ is a temperature-dependent reaction rate constant, $f(\alpha)$ is the differential conversion function depending on the reaction mechanism, and $\beta = dT/dt$ is a constant heating rate.

The DSC curves were analyzed on the basis of the following assumption: the exothermic heat evolved during curing is proportional to the conversion of monomer to polymer. The degree of curing, α, is determined by the following equations:

$$\alpha = \frac{\Delta H_i}{\Delta H_o} \quad (2)$$

$$\Delta H_i = \int_0^t \frac{dH}{dt}\, dt \quad (3)$$

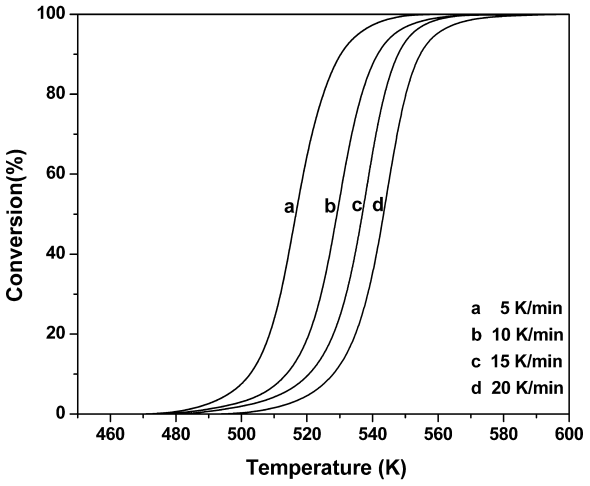

Fig. 4. Conversion α as a function of temperature for the BEF-p in different heating rates.

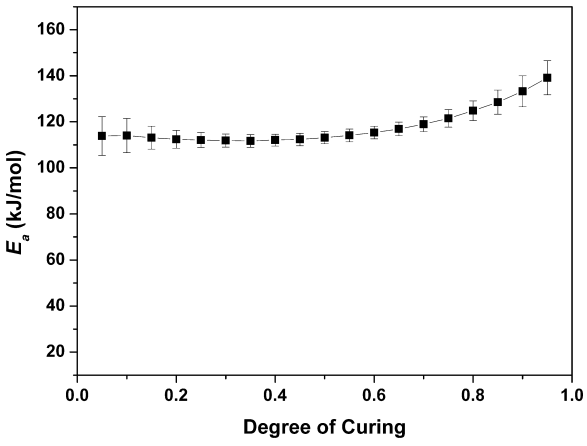

Fig. 5. Variation of E_a vs. α by Starink method.

where ΔH_i is the total amount of heat evolved by the reaction from the beginning to time t. ΔH_o is the total heat of curing reaction.

The temperature dependence on the rate constant is typically represented through the Arrhenius equation:

$$k(T) = A \ \exp\left(\frac{-E_a}{RT}\right) \tag{4}$$

where A is the pre-exponential factor. E_a is the activation energy, which can be determined by Arrhenius law without assuming the kinetic model function. R is the universal gas constant, and T is the absolute temperature.

Combining Eq. (1) with Eq. (4) it results:

$$\frac{d\alpha}{dt} = \beta\frac{d\alpha}{dT} = A \ \exp\left(\frac{-E_a}{RT}\right) f(\alpha) \tag{5}$$

Non-isothermal method, more accurate to determine the curing kinetic parameters, is carried out at different heating rates. In addition, this method is very attractive because the kinetic data can be obtained in a relatively short period of time [55]. In this work, a multiple-heating-rate method for dynamic mode was used to evaluate the polymerization reaction kinetic parameters. Fig. 4 shows the variation of the degree of conversion (α) as a function of curing temperature obtained from dynamic DSC.

The kinetic parameters of the curing reaction, with special reference to E_a, can be calculated using various computational methods. An alternative approach to kinetic analysis is to use model-free methods that allow the evaluating of Arrhenius parameters without choosing the reaction model. The best known representatives of the model-free approach are the isoconversional methods [62,63]. These methods are based on the isoconversional principle which states that the reaction rate at a constant extent of conversion is only a function of the temperature. They can generally be split in two categories: differential and integral methods. The differential isoconversional method presents the most straightforward way to evaluate the effective activation energy, E_a, as a function of the extent of reaction. This method can be applied to integral data (e.g. TG data) only after their numerical differentiation. Because this procedure may lead to erroneous estimations of the activation energy, the use of the integral isoconversional methods appears to be a safer alternative [62]. For non-isothermal conditions, the activation energy can be calculated by various integral isoconversional methods such as Ozawa, Kissinger, Starink methods. Compared to these methods, Straink method offers a significant improvement in the accuracy of the E_a values [61]. In this work, the average activation energy value obtained from Starink method was used for the determination of the reaction order of the BEF-p. This method is based on Eq. (6) [64].

$$\ln\left(\frac{\beta}{T_f^{1.92}}\right) = \text{Const.} - 1.0008\,\frac{E_a}{RT_f} \tag{6}$$

where T_f is the temperature at an equivalent (fixed) state of transformation in different heating rate.

From Eq. (6), a plot of $\ln(\beta/T_f^{1.92})$ vs. $1/T_f$ values at the same fractional extent of conversion from a series of dynamic DSC experiments at different heating rates would result in a straight line with a slope of $-1.0008E_a/R$. Repeating this procedure, the E_a values corresponding to different α from the DSC curing curves at different heating rates can be obtained. The plot of activation energy as a function of conversion was shown in Fig. 5. It could be clearly seen that the activation energy values tended to increase with the degree of conversion. And, the average value of the activation energy of BEF-p is 117.9 ± 4.2 kJ/mol.

According to the experimental data and the average activation energy value obtained from Starink method, we can produce the plots of $\ln(d\alpha/dt) + E_a/RT$ vs. $\ln(1-\alpha)$ as shown in Fig. 6. In Fig. 6, the peak points of the lines correspond to the peak point of the DSC curve. It is observed that there is a nonlinear increase before the peak points and a linear decrease after them. In the n-order model, the reaction rate is the highest at the beginning of curing, and it decreases as the reaction proceeds. For autocatalytic process, the plot would show a maximum of $\ln(1-\alpha)$ approximately

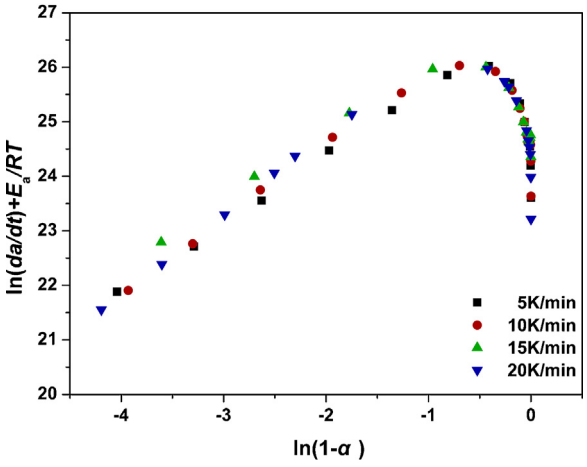

Fig. 6. The plots of $\ln d\alpha/dt + E_a/RT$ vs. $\ln(1-\alpha)$ for different heating rates.

in the range of −0.51 to −0.22, which is equivalent to degree of curing of about 0.2–0.4. This is due to the autocatalytic nature that shows the maximum reaction rate at 20–40% conversion [65–67]. Since $\ln(d\alpha/dt)+E_a/RT$ and $\ln(1-\alpha)$ were not linearly related and evidently showed a maximum in the range of the degree of conversion mentioned above, this suggested that the curing reaction was autocatalytic in nature. According to other works, the autocatalytic nature of reaction kinetics of benzoxazine can be explained by the generation of free phenol groups while the benzoxazine ring starts to open. These groups can further accelerate the ring opening process [53,54].

For the benzoxazine resins, autocatalytic model (Šesták–Berggren equation) assumes that the reaction obeys equation:

$$f(\alpha) = \alpha^m (1-\alpha)^n \tag{7}$$

Combined with Eq. (5) and Eq. (7), the kinetic model can be described as follows:

$$\frac{d\alpha}{dt} = \beta\frac{d\alpha}{dT} = A\ \exp\left(\frac{-E_a}{RT}\right)\alpha^m(1-\alpha^n) \tag{8}$$

where m and n are variables determining the reaction order.

The method of least square regression (LSR) assumes that the best fit curve of a given type is the curve that has the minimal sum of the deviations squared (least square error) from a given set of data. This method is used to deal with the non-isothermal DSC data in order to obtain the optimum model parameters [68]. Theoretically, Eq. (8) could be solved by multiple nonlinear regressions. Because the cure rate was an exponential function of the reciprocal of the absolute temperature, it was difficult to get a good solution. The fitting results showed that large errors exist for the kinetic parameters obtained by such a method. By taking the logarithm of both sides of Eq. (8), a linear expression for the logarithm of cure rate can be obtained:

$$\ln\left(\frac{d\alpha}{dt}\right) = \ln\left(\beta\frac{d\alpha}{dT}\right) = \ln A - \left(\frac{E_a}{RT}\right) + m\ \ln(\alpha) + n\ \ln(1-\alpha) \tag{9}$$

Eq. (9) can be solved by multiple linear regression using the several different heating rates of data at the same time, in which the dependent variable is $\ln[\beta(d\alpha/dT)]$, and the independent variables are $\ln\alpha$, $\ln(1-\alpha)$, and $1/T$. Therefore, the values of A, m, and n can be obtained using the average activation energy from Starink method. The degree of curing is chosen to range between $\alpha = 0.05$ and 0.95.

In all cases, the thermograms obtained at different heating rates were simultaneously correlated with the same set of kinetic parameters. In this way a single set of kinetic parameters is obtained to fit all the experimental data and no variation of these parameters at the heating rate is required. Using this method, the kinetic parameters are gained: $E_a \approx 117.9 \pm 4.2$ kJ/mol, $m \approx 0.93$, $n \approx 1.45$, $A \approx \exp(27.59)$, respectively. Thus, the curing kinetic equation of the BEF-p can be expressed as:

$$\frac{d\alpha}{dt} = \beta\frac{d\alpha}{dT} = \exp(27.59)\exp\left(\frac{-14174}{T}\right)\alpha^{0.93}(1-\alpha)^{1.45} \tag{10}$$

The experimental curves and predicted curves based on the determined kinetic parameters of curing reaction were shown in Fig. 7. It could be clearly seen that the calculated data from the model were in good agreement with the experimental results.

For the calculated kinetic parameters described above, we first need to get E_a, and kinetic parameters cannot be obtained simultaneously. Therefore, we will discuss another least square regression method, which is used to deal with the non-isothermal DSC data in order to determine the optimum model parameters [68]. In this method, the values of E_a, n, m and $\ln A$ can be calculated by multiple linear regression model (Eq. (9)), where $\ln\alpha$, $\ln(1-\alpha)$, and $1/T$ are the independent variable and $\ln[\beta(d\alpha/dT)]$ is the dependent variable.

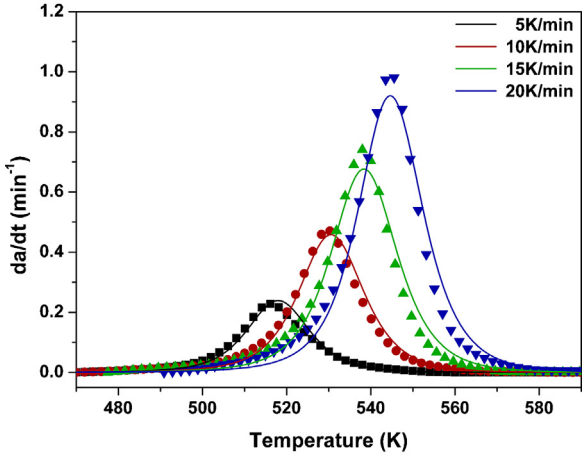

Fig. 7. Comparison of experimental values (symbols) and calculated values (lines) by Starink-LSR method.

The results of the multiple linear regressions analysis of BEF-p are $E_a \approx 127.8 \pm 2.2$ kJ/mol, $m \approx 0.89$, $n \approx 1.47$, $A \approx \exp(29.87)$. The curing kinetic equation of the BEF-p with this least square regression (LSR) method can be expressed as:

$$\frac{d\alpha}{dt} = \beta\frac{d\alpha}{dT} = \exp(29.87)\exp\left(-\frac{15381}{T}\right)\alpha^{0.89}(1-\alpha)^{1.47} \tag{11}$$

The comparisons of the experimental data with the kinetic model are shown in Fig. 8. The calculated curves were compared with the experimental curves, and were found to be similar to the experimental curves.

3.4. Thermal and mechanical properties of polybenzoxazines

Thermal properties of BEF-p after polymerization have been investigated in comparison to the typical fluorene diamine-based polybenzoxazine (poly(BF-p)) derived from 9,9-bis-(4-aminophenyl)-fluorene/phenol bifunctional benzoxazine (BF-p) without aryl ether [39]. The T_g of poly(BEF-p) was obtained by DSC and DMA, and shown in Figs. 3 and 9, respectively. As a result, the T_g value of poly(BEF-p) reaches 240 °C by DSC and 253 °C by DMA, respectively, and is 3 °C lower than that of poly(BF-p), but is much higher than that of the diaminodiphenylmethane-based polybenzoxazine (P-ddm, 200 °C by DMA) and bisphenol fluorene-aniline-based polybenzoxazine (poly(B-pbf), 229 °C by DSC) [17,34]. This is mainly attributed to the backbone rigidity

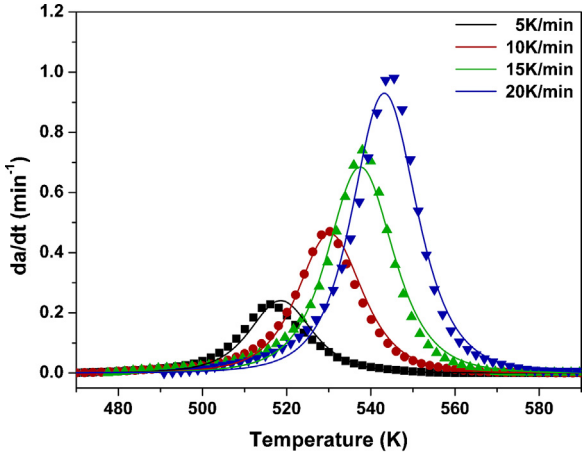

Fig. 8. Comparison of experimental values (symbols) and calculated values (lines) by direct LSR method.

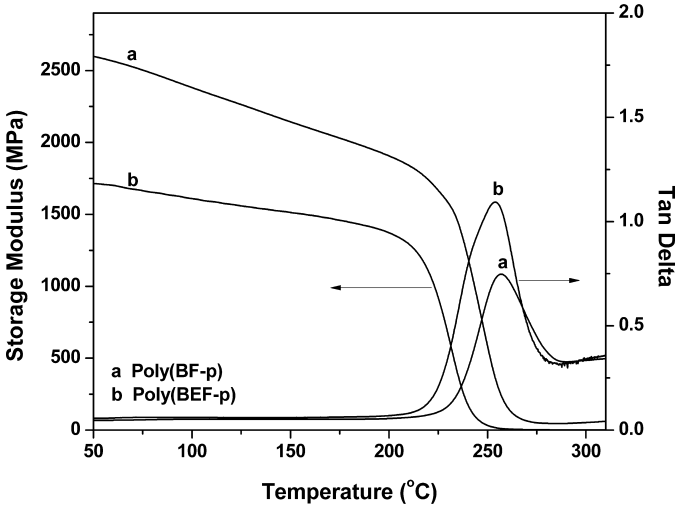

Fig. 9. Temperature dependence curves of storage modulus and tan delta for poly(BEF-p) and poly(BF-p).

of polybenzoxazine molecule. Bulky fluorene units have the high rigidity in the chain backbone, which restrain the internal rotations and thermal motion of polymer segments. Furthermore, the storage modulus of poly(BEF-p) is about 1.7 GPa, which is much lower than that of poly(BF-p) (2.6 GPa). The result shows that the stiffness of polybenzoxazine observably decreases due to the introduction of flexible ether linkages, and the brittleness of fluoren-containing polybenzoxazine is greatly improved.

Thermal stability was evaluated by thermogravimetric analyses (TGA) under nitrogen atmosphere. As can be seen in Fig. 10, the temperatures corresponding to 5% and 10% weight loss (T_5 and T_{10}) are 388 and 420 °C, respectively, which are slightly lower than that of poly(BF-p) (401 and 432 °C for T_5 and T_{10}, respectively), but much higher than that of poly(B-pbf) (334 and 364 °C, respectively). The char yield (Y_c) at 800 °C is 49%, which is closed to that of poly(BF-p) and poly(B-pbf) (47% and 51%, respectively) [34,39]. This result indicated that the incorporation of flexible aryl ether linkages into macromolecular backbone had a little influence on the thermal stability of fluorene-containing polybenzoxazine.

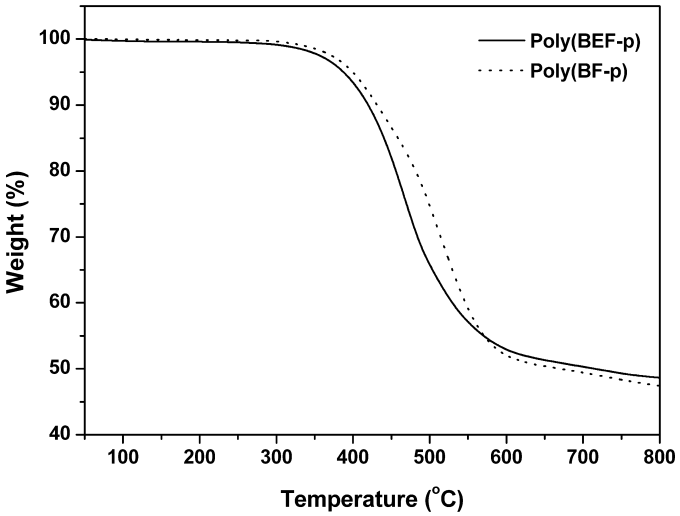

Fig. 10. TGA thermograms of the cured poly(BEF-p) and poly(BF-p) under nitrogen.

4. Conclusions

The fluorene diamine-based benzoxazine with aryl ether linkages has been prepared and characterized. The polymerization behavior, mechanical and thermal properties were studied by DSC, FT-IR, DMA and TGA. With the introduction of bulky fluorenyl moieties, poly(BEF-p) exhibits higher glass transition temperature and thermal stability than those of P-ddm and bisphenol fluorene-based polybenzoxazines. Incorporation of flexible aryl ether linkages into fluorene-based polybenzoxazine slightly affects the thermal stability of poly(BEF-p), however, the brittleness of polybenzoxazine is greatly modified compared with poly(BF-p). The curing kinetics of BEF-p was investigated using non-isothermal DSC methods. Autocatalytic model (Šesták–Berggren equation) was used to describe the cure kinetic phenomena of BEF-p. The model parameters were estimated by Starink-LSR method and direct LSR method. The theoretically calculated curves show a good agreement with the experimental data. In addition, the kinetic parameters can be simultaneously obtained from direct LSR method.

Acknowledgements

This work has been funded by the financial supports from National Natural Science Foundation of China (Project no. 50973022), Specialized Research Fund for the Doctoral Program of Higher Education (Project no. 20122304110019), Fundamental Research Funds for the Central Universities (Project nos. HEUCFT1009, HEUCFR1227, 201310006), Natural Science Foundation of Heilongjiang Province (Project no. E200921), and Innovation Foundation of Harbin (Project no. 2010RFXXG008).

References

[1] X. Ning, H. Ishida, Phenolic materials via ring-opening polymerization: synthesis and characterization of bisphenol-A based benzoxazines and their polymers, J. Polym. Sci. Part A: Polym. Chem. 32 (1994) 1121–1129.
[2] X. Ning, H. Ishida, Phenolic materials via ring-opening polymerization of benzoxazines: effect of molecular structure on mechanical and dynamic mechanical properties, J. Polym. Sci. Part B: Polym. Phys. 32 (1994) 921–927.
[3] H. Ishida, D.J. Allen, Physical and mechanical characterization of near-zero shrinkage polybenzoxazines, J. Polym. Sci. Part B: Polym. Phys. 34 (1996) 1019–1030.
[4] A. Laobuthee, S. Chirachanchai, H. Ishida, K. Tashiro, Asymmetric monooxazine: an inevitable product from Mannich reaction of benzoxazine dimers, J. Am. Chem. Soc. 123 (2001) 9947–9955.
[5] N.N. Ghosh, B. Kiskan, Y. Yagci, Polybenzoxazines – new high performance thermosetting resins: synthesis and properties, Prog. Polym. Sci. 32 (2007) 1344–1391.
[6] T. Agag, T. Takeichi, Novel benzoxazine monomers containing p-phenyl propargyl ether: polymerization of monomers and properties of polybenzoxazines, Macromolecules 34 (2001) 7257–7263.
[7] T. Agag, T. Takeichi, Synthesis and characterization of novel benzoxazine monomers containing allyl groups and their high performance thermosets, Macromolecules 36 (2003) 6010–6017.
[8] Z. Brunovska, R. Lyon, H. Ishida, Thermal properties of phthalonitrile functional polybenzoxazines, Thermochim. Acta 357 (2000) 195–203.
[9] H. Ishida, S. Ohba, Synthesis and characterization of maleimide and norbornene functionalized benzoxazines, Polymer 46 (2005) 5588–5595.
[10] Y.C. Su, F.C. Chang, Synthesis and characterization of fluorinated polybenzoxazine material with low dielectric constant, Polymer 44 (2003) 7989–7996.
[11] H. Kimura, Y. Murata, A. Matsumoto, K. Hasegawa, K. Ohtsuka, A. Fukuda, New thermosetting resin from terpenediphenol-based benzoxazine and epoxy resin, J. Appl. Polym. Sci. 74 (1999) 2266–2273.
[12] A.W. Kawaguchi, A. Sudo, T. Endo, Synthesis of highly polymerizable 1,3-benzoxazine assisted by phenyl thio ether and hydroxyl moieties, J. Polym. Sci. Part A: Polym. Chem. 50 (2012) 1457–1461.
[13] D.J. Allen, H. Ishida, Effect of phenol substitution on the network structure and properties of linear aliphatic diamine-based benzoxazines, Polymer 50 (2009) 613–626.
[14] D.J. Allen, H. Ishida, Polymerization of linear aliphatic diamine-based benzoxazine resins under inert and oxidative environments, Polymer 48 (2007) 6763–6772.
[15] C.H. Lin, S.L. Chang, C.W. Hsieh, H.H. Lee, Aromatic diamine-based benzoxazines and their high performance thermosets, Polymer 49 (2008) 1220–1229.

[16] C.H. Lin, H.T. Lin, J.W. Sie, K.Y. Hwang, A.P. Tu, Facile, one-pot synthesis of aromatic diamine-based phosphinated benzoxazines and their flame-retardant thermosets, J. Polym. Sci. Part A: Polym. Chem. 48 (2010) 4555–4566.
[17] S.L. Chang, C.H. Lin, Facile, one-pot synthesis of aromatic diamine-based benzoxazines and their advantages over diamines as epoxy hardeners, J. Polym. Sci. Part A: Polym. Chem. 48 (2010) 2430–2437.
[18] T. Agag, L. Jin, H. Ishida, A new synthetic approach for difficult benzoxazines: Preparation and polymerization of 4,4′-diaminodiphenyl sulfone-based benzoxazine monomer, Polymer 50 (2009) 5940–5944.
[19] W. Men, Z. Lu, Synthesis and characterization of 4,4′-diaminodiphenyl methane-based benzoxazines and their polymers, J. Appl. Polym. Sci. 106 (2007) 2769–2774.
[20] Y.L. Liu, C.W. Hsu, C.I. Chou, Silicon-containing benzoxazines and their polymers: copolymerization and copolymer properties, J. Polym. Sci. Part A: Polym. Chem. 45 (2007) 1007–1015.
[21] M. Sponton, M.S. Larrechi, J.C. Ronda, M. Galia, V. Cadiz, Synthesis and study of the thermal crosslinking of bis(m-aminophenyl) methylphosphine oxide based benzoxazine, J. Polym. Sci. Part A: Polym. Chem. 46 (2008) 7162–7172.
[22] C.H. Lin, S.L. Chang, H.H. Lee, H.C. Chang, K.Y. Hwang, A.P. Tu, W.C. Su, Fluorinated benzoxazines and the structure-property relationship of resulting polybenzoxazines, J. Polym. Sci. Part A: Polym. Chem. 46 (2008) 4970–4983.
[23] A. Chernykh, T. Agag, H. Ishida, Novel benzoxazine monomer containing diacetylene linkage: an approach to benzoxazine thermosets with low polymerization temperature without added initiators or catalysts, Polymer 50 (2009) 3153–3157.
[24] L. Jin, T. Agag, H. Ishida, Bis(benzoxazine-maleimide)s as a novel class of high performance resin: synthesis and properties, Eur. Polym. J. 46 (2010) 354–363.
[25] S. Rimdusit, S. Tiptipakorn, C. Jubsilp, T. Takeichi, Polybenzoxazine alloys and blends: some unique properties and applications, React. Funct. Polym. 73 (2013) 369–380.
[26] M. Fakis, F. Zacharatos, V. Gianneta, P. Persephonis, V. Giannetas, A. Nassiopoulou, Photoluminescence properties of porous silicon/fluorene dye composites, Mater. Sci. Eng. B 165 (2009) 252–255.
[27] S.C. Lin, E.M. Pearce, Epoxy resins. II. The preparation, characterization, and curing of epoxy resins and their copolymers, J. Polym. Sci. Part A: Polym. Chem. Ed. 17 (1979) 3095–3119.
[28] W. Liu, Q. Qiu, J. Wang, Z. Huo, H. Sun, Curing kinetics and properties of epoxy resin–fluorenyl diamine systems, Polymer 49 (2008) 4399–4405.
[29] T.A. Reddy, M. Srinivasan, Preparation and properties of cardopolyimides containing phenoxaphosphine units, J. Polym. Sci. Part A: Polym. Chem. 27 (1989) 1419–1424.
[30] S.H. Hsiao, C.T. Li, Synthesis and characterization of new fluorene-based poly(ether imide)s, J. Polym. Sci. Part A: Polym. Chem. 37 (1999) 1403–1412.
[31] A.D. Sagar, R.D. Shingte, P.P. Wadgaonkar, M.M. Salunkhe, Polyamides containing s-triazine rings and fluorene "cardo" groups: synthesis and characterization, Eur. Polym. J. 37 (2001) 1493–1498.
[32] M. Nishikawa, Design of polyimides for liquid crystal alignment films, Polym. Adv. Technol. 11 (2000) 404–412.
[33] P.R. Srinivasan, V. Mahadevan, M. Srinivasan, Preparation and properties of some cardopolyamides, J. Polym. Sci. Part A: Polym. Chem. Ed. 19 (1981) 2275–2285.
[34] J. Wang, M.Q. Wu, W.B. Liu, S.W. Yang, J.W. Bai, Q.Q. Ding, Y. Li, Synthesis, curing behavior and thermal properties of fluorene containing benzoxazines, Eur. Polym. J. 46 (2010) 1024–1031.
[35] Y.L. Liu, C.Y. Chang, C.Y. Hsu, M.C. Tseng, C.I. Chou, Preparation, characterization, and properties of fluorene-containing benzoxazine and its corresponding cross-linked polymer, J. Polym. Sci. Part A: Polym. Chem. 48 (2010) 4020–4026.
[36] Y. Lu, M. Li, Y. Zhang, D. Hu, L. Me, W. Xu, Synthesis and curing kinetics of benzoxazine containing fluorene and furan groups, Thermochim. Acta 515 (2011) 32–37.
[37] Z. Fu, H. Liu, H. Cai, X. Liu, G. Ying, K. Xu, M. Chen, Synthesis, thermal polymerization, and properties of benzoxazine resins containing fluorenyl moiety, Polym. Eng. Sci. 52 (2012) 2473–2481.
[38] H.C. Chang, C.H. Lin, Y.W. Tian, Y.R. Feng, L.H. Chan, Synthesis of 9,9-bis(4-aminophenyl)fluorene-based benzoxazine and properties of its high-performance thermoset, J. Polym. Sci. Part A: Polym. Chem. 50 (2012) 2201–2210.
[39] J. Wang, X.Y. He, J.T. Liu, W.B. Liu, L. Yang, Investigation of the Polymerization behavior and regioselectivity of fluorene diamine-based benzoxazines, Macromol. Chem. Phys. 214 (2013) 617–628.
[40] T. Takeichi, Y. Guo, S. Rimdusit, Performance improvement of polybenzoxazine by alloying with polyimide: effect of preparation method on the properties, Polymer 46 (2005) 4909–4916.
[41] H. Ishida, D.J. Allen, Mechanical characterization of copolymers based on benzoxazine and epoxy, Polymer 37 (1996) 4487–4495.
[42] K.S. Santhosh Kumar, C.P. Reghunadhan Nair, K.N. Ninan, Investigations on the cure chemistry and polymer properties of benzoxazine–cyanate ester blends, Eur. Polym. J. 45 (2009) 494–502.
[43] T. Takeichi, Y. Guo, T. Agag, Synthesis and characterization of poly(urethane–benzoxazine) films as novel type of polyurethane/phenolic resin composites, J. Polym. Sci. Part A: Polym. Chem. 38 (2000) 4165–4176.
[44] M.R. Vengatesan, S. Devaraju, D. Kannaiyan, J.K. Song, M. Alagar, Ultrasound-assisted synthesis of benzoxazine monomers: thermal and mechanical properties of polybenzoxazines, Polym. Int. 62 (2013) 127–133.
[45] P. Kasemsiri, S. Hiziroglu, S. Rimdusit, Effect of cashew nut shell liquid on gelation, cure kinetics, and thermomechanical properties of benzoxazine resin, Thermochim. Acta 520 (2011) 84–92.
[46] B. Lochab, I. Varma, J. Bijwe, Thermal behaviour of cardanol-based benzoxazines, J. Therm. Anal. Calorim. 102 (2010) 769–774.
[47] C.P. Yang, J.H. Lin, Syntheses and properties of aromatic polyamides and polyimides derived from 9,9-bis[4-(p-aminophenoxy)phenyl]fluorene, J. Polym. Sci. Part A: Polym. Chem. 31 (1993) 2153–2163.
[48] C.P. Yang, J.H. Lin, Preparation and properties of aromatic polyamides and polyimides derived from 3,3-bis [4-(4-aminophenoxy) phenyl] phthalide, J. Polym. Sci. Part A: Polym. Chem. 32 (1994) 423–433.
[49] S.H. Hsiao, C.P. Yang, W.L. Lin, Synthesis and characterization of new diphenylfluorene-based aromatic polyamides derived from 9,9-bis[4-(4-carboxy -phenoxy)phenyl]fluorene, Macromol. Chem. Phys. 200 (1999) 1428–1433.
[50] C.P. Yang, S.H. Hsiao, K.L. Wu, Organosoluble and light-colored fluorinated polyimides derived from 2,3-bis(4-amino-2-trifluoromethylphenoxy)naphthalene and aromatic dianhydrides, Polymer 44 (2003) 7067–7078.
[51] C.P. Yang, H.C. Chiang, Organosoluble and light-colored fluorinated polyimides based on 9,9-bis[4-(4-amino-2-trifluoromethylphenoxy)phenyl]fluorene and aromatic dianhydrides, Colloid. Polym. Sci. 282 (2004) 1347–1358.
[52] J. Wang, X. Fang, M.Q. Wu, X.Y. He, W.B. Liu, X.D. Shen, Synthesis, curing kinetics and thermal properties of bisphenol-AP-based benzoxazine, Eur. Polym. J. 47 (2011) 2158–2168.
[53] H. Ishida, Y. Rodriguez, Curing kinetics of a new benzoxazine-based phenolic resin by differential scanning calorimetry, Polymer 36 (1995) 3151–3158.
[54] H. Ishida, Y. Rodriguez, Catalyzing the curing reaction of a new benzoxazine-based phenolic resin, J. Appl. Polym. Sci. 58 (1995) 1751–1760.
[55] C. Jubsilp, S. Damrongsakkul, T. Takeichi, S. Rimdusit, Curing kinetics of arylamine-based polyfunctional benzoxazine resins by dynamic differential scanning calorimetry, Thermochim. Acta 447 (2006) 131–140.
[56] Y. Liu, Z. Yue, J. Gao, Synthesis, characterization, and thermally activated polymerization behavior of bisphenol-S/aniline based benzoxazine, Polymer 51 (2010) 3722–3729.
[57] W.S. Chow, S. Grishchuk, T. Burkhart, J. Karger-Kocsis, Gelling and curing behaviors of benzoxazine/epoxy formulations containing 4,4′-thiodiphenol accelerator, Thermochim. Acta 543 (2012) 172–177.
[58] C. Andronescu, S.A. Garea, C. Deleanu, H. Iovu, Characterization and curing kinetics of new benzoxazine monomer based on aromatic diamines, Thermochim. Acta 530 (2012) 42–51.
[59] W. Liu, J. Wang, Q. Qiu, L. Ji, C. Wang, M. Zhang, Synthesis and characterisation of 9,9-bis (4-hydroxyphenyl)-fluorene catalysed by cation exchanger, Pigment Resin Technol. 37 (2008) 9–15.
[60] J. Dunkers, H. Ishida, Vibrational assignments of 3-alkyl-3,4-dihydro-6-methyl-2H-1,3-benzoxazines in the fingerprint region, Spectrochim. Acta A 51A (1995) 1061–1074.
[61] S. Vyazovkin, A.K. Burnham, J.M. Criado, L.A. Pérez-Maqueda, C. Popescu, N. Sbirrazzuoli, ICTAC kinetics committee recommendations for performing kinetic computations on thermal analysis data, Thermochim. Acta 520 (2011) 1–19.
[62] S. Vyazovkin, Computational aspects of kinetic analysis. Part C. The ICTAC kinetics project – the light at the end of the tunnel? Thermochim. Acta 355 (2000) 155–163.
[63] J. Wang, H. Wang, J. Liu, W. Liu, X. Shen, Synthesis, curing kinetics and thermal properties of novel difunctional chiral and achiral benzoxazines with double chiral centers, J. Therm. Anal. Calorim. (2013), http://dx.doi.org/10.1007/s10973-013-3081-8.
[64] M.J. Starink, The determination of activation energy from linear heating rate experiments: a comparison of the accuracy of isoconversion methods, Thermochim. Acta 404 (2003) 163–176.
[65] L. Ke, D. Hu, Y. Lu, S. Feng, Y. Xie, W. Xu, Copolymerization of maleimide-based benzoxazine with styrene and the curing kinetics of the resultant copolymer, Polym. Degrad. Stab. 97 (2012) 132–138.
[66] C. Jubsilp, K. Punson, T. Takeichi, S. Rimdusit, Curing kinetics of benzoxazine-epoxy copolymer investigated by non-isothermal differential scanning calorimetry, Polym. Degrad. Stab. 95 (2010) 918–924.
[67] T.H. Hsieh, A.C. Su, Cure kinetics of an epoxy-novolac molding compound, J. Appl. Polym. Sci. 41 (1990) 1271–1280.
[68] J. Zhang, H. Dong, L. Tong, L. Meng, Y. Chen, G. Yue, Investigation of curing kinetics of sodium carboxymethyl cellulose/epoxy resin system by differential scanning calorimetry, Thermochim. Acta 549 (2012) 63–68.